

# Analytical Methods

Accepted Manuscript



This is an *Accepted Manuscript*, which has been through the Royal Society of Chemistry peer review process and has been accepted for publication.

*Accepted Manuscripts* are published online shortly after acceptance, before technical editing, formatting and proof reading. Using this free service, authors can make their results available to the community, in citable form, before we publish the edited article. We will replace this *Accepted Manuscript* with the edited and formatted *Advance Article* as soon as it is available.

You can find more information about *Accepted Manuscripts* in the [Information for Authors](#).

Please note that technical editing may introduce minor changes to the text and/or graphics, which may alter content. The journal's standard [Terms & Conditions](#) and the [Ethical guidelines](#) still apply. In no event shall the Royal Society of Chemistry be held responsible for any errors or omissions in this *Accepted Manuscript* or any consequences arising from the use of any information it contains.

## Mechanistic evaluation of the size dependent antimicrobial activity of water soluble QDs

Aakriti Tyagi<sup>1</sup>, Kamla Rawat<sup>2,3</sup>, Anita K. Verma<sup>1\*</sup> and H. B. Bohidar<sup>2,4\*</sup>

<sup>1</sup>Nanobiotech Lab, Dept of Zoology, Kirori Mal College, University of Delhi, India

<sup>2</sup>Special Centre for Nano Sciences, Jawaharlal Nehru University, New Delhi, India

<sup>3</sup>Inter University Accelerator Centre (IUAC), New Delhi, India

<sup>4</sup>School of Physical Sciences, Jawaharlal Nehru University, New Delhi, India

Corresponding Author Email: [bohi0700@mail.jnu.ac.in](mailto:bohi0700@mail.jnu.ac.in); [akamra23@hotmail.com](mailto:akamra23@hotmail.com)

Fax: +91 11 2674 1837; Tel: +91 11 2674 4637/4699

### Abstract

Herein, we report preparation of water soluble CdSe quantum dots (coated with 3-mercaptopropionic acid, MPA) of variable size (2.43-5.09 nm) based on hot injection kinetic synthesis. A comprehensive spectroscopic analysis of these nanoparticles by steady state and time resolved fluorescence spectroscopy yielded interesting results. Since the internalization of QDs by prokaryotes has not been well-understood, as yet, the activity of the variable sized QDs was assessed against *Escherichia coli* DH5 $\alpha$  (gram-negative) and *Staphylococcus aureus* (gram-positive bacteria), ATCC 13709 by agar disc assay and MTT assay. The mechanisms of toxicity were evaluated by measuring the reactive oxygen species (ROS) generated by the QDs alone and investigating the oxidative damage to bacteria. The sensitivity of *S. aureus* was higher compared to *E. coli* and a significant size dependent increase in intracellular ROS generation compared to control was noted. Statistically significant size-dependent increase in the Zone of inhibition was observed in *S. aureus* and *E. coli* by Agar disc diffusion assay.

Since, reduced glutathione (GSH) is the primary line of defence against acute toxicities of electrophiles and ROS and has a detrimental role in conferring cellular protection, hence the GSH depletion was quantified. GSH in *S. aureus* and *E. coli* by QD-A (2.43 nm =  $0.055 \pm 0.0007$ ,  $0.053 \pm 0.0002$ ), QD-C (5.09 nm =  $0.057 \pm 0.001$ ,  $0.054 \pm 0.0046$ ) followed by QD-B (3.75 nm =  $0.060 \pm 0.0003$ ,  $0.057 \pm 0.0005$ ) with respect to control ( $0.086 \pm 0.001$ ,  $0.075 \pm 0.0005$ ). ROS was further quantified using DCFH-DA. An increase in the levels of reactive oxygen species [QD-A treatment ( $119.35\% \pm 5.77\%$  and  $34.58\% \pm 5.77\%$ ), QD-C ( $62.90\% \pm$

1  
2  
3 11.54% and  $23.3\% \pm 5.77\%$ ) followed by QD-B ( $14.51\% \pm 15.27\%$  and  $12.03\% \pm 5.77\%$ ).  
4  
5 Lactate dehydrogenase release determines the integrity of cell membrane and the LDH release  
6  
7 was directly proportional to cellular damage [QD-A ( $104.05\% \pm 5.77\%$  and  $102.61\% \pm 13.76\%$ )  
8  
9 and C ( $68.89\% \pm 7.21\%$  and  $29.4\% \pm 15.12\%$ ) followed by B ( $51.68\% \pm 11.54\%$  and  $18.45\% \pm$   
10  
11  $15.46\%$ )]. The QDs induced oxidative stress enhanced genotoxicity as evidenced by the DNA  
12  
13 damage in *S. aureus* (QD-A>QD-C>QD-B =  $53\% \pm 1.5\%$ ,  $49\% \pm 1.15\%$  ,  $47\% \pm 1.15\%$ ) and *E.*  
14  
15 *coli* ( $49.5\% \pm 1.73\%$  ,  $45\% \pm 0.57\%$  ,  $42\% \pm 1.15\%$ ). Results confirmed the role of QDs in  
16  
17 inducing oxidative stress in microbial system whereby it can be applied to inflict damage to  
18  
19 many unwanted members of the microbial communities.

20 Key words: Water soluble QDs, Cytotoxicity, Antimicrobial properties, LDH, ROS, DNA  
21  
22 fragmentation.  
23  
24  
25  
26  
27  
28  
29  
30  
31  
32  
33  
34  
35  
36  
37  
38  
39  
40  
41  
42  
43  
44  
45  
46  
47  
48  
49  
50  
51  
52  
53  
54  
55  
56  
57  
58  
59  
60

## 1. Introduction

Biological applications of semiconductor quantum dots (QDs) have gained considerable attention in the recent past. This is because semiconductor nanocrystals, quantum dots, are promising nanomaterials, which have found applications in many areas such as photonics, pharmaceuticals, semiconductor devices etc. The remarkable features of QDs are: possession of broad absorption and narrow emission bands, exhibition of size-tunable colour, and presence of large two-photon absorption cross-section.<sup>1, 2</sup> QDs solutions exhibit visible colour changes even by minuscule variations in the radius of QDs. This property may be used to exploit their potential for concurrent multiple colour labels<sup>3, 4, 5</sup> The size differences majorly affect their uptake that may lead to modifications in cellular activity and cytotoxicity.<sup>6</sup> Further, applications in biology and pharmaceuticals as drug/gene carriers, and imaging agents require water-solubility of this luminescent quantum dots.<sup>7-9</sup> Strong interaction of nanoparticles with intra-cellular proteins may cause transmission of biological signals owing to altered protein conformation. This altered signal transduction in cells may cause toxicity. Of the quantum dots available, CdSe stands out as a promising candidate because its optical band gap is dependent on its particle size. The conversion of these QDs from their hydrophobic state to hydrophilic nature is necessary, which is achieved by a phase-transfer process.<sup>10</sup> However, such a process causes the resultant particles to have limited stability due to tendency to grow in size, and poor photoluminescence efficiency.<sup>11</sup> Size-dependent photoluminescence (PL) spectral profile spanning the broad visible region of the electromagnetic spectrum<sup>12, 13</sup> has facilitated the extensive use of 3-mercaptopropionic acid (MPA)-capped Cadmium Selenide (CdSe) QDs in biology particularly in cellular labelling, and imaging applications.

Of the two component ions  $\text{Cd}^{+2}$  and  $\text{Se}^{-2}$ ,  $\text{Cd}^{+2}$  belongs to the heavy metal group, and the consolidated impact of these ions on plasma proteins is poorly understood. The hydrophobic nature of CdSe nanoparticles requires surface modification to enable these to be hydrophilic (achievable through ligand exchange). In the past, capping agents belonging to both the organic and inorganic compounds like polymers, amines, tri-n-octyl phosphine oxide (TOPO) and thiols were used. Moreover, such surface capping prevents non-radiative recombination at the surface sites, and raises the coagulation barrier, inhibiting aggregation due to steric hindrance<sup>14</sup>. It is important to note that the QD interface environment (capping) has specific property that plays significant role in determining its spectroscopic signature like luminescence.<sup>11</sup> In particular, the

1  
2  
3 water-soluble and biocompatible QDs have found use in a wide range of applications spanning  
4 pharmaceuticals, cellular imaging etc.<sup>16, 17</sup> Peng et al have comprehensively analyzed the cellular  
5 uptake, elimination and toxicity of four CdSe/ZnS QDs in HepG2 cells by using high sensitive  
6 and element-selective ICP-MS measurement, MTT assay, AO/EB staining, and glutathione level  
7 and gene expression analysis. This work provides a systematic assay for the evaluation of the  
8 cytotoxicity of specific QDs, based on a variety of chemical and biological technologies, and the  
9 obtained results can be correlated<sup>18</sup>.

10  
11  
12 Herein, we have conducted a systematic and comprehensive study to understand size  
13 dependent toxicity and antimicrobial properties of MPA capped QDs. There are limited number  
14 of experimental studies devoted to size dependent cytotoxicity, and antimicrobial efficacy of  
15 QDs reported in the literature. Therefore, our knowledge of size dependent interaction of these  
16 moieties with cells and microbes remain poorly understood which has motivated the present  
17 work.

## 18 19 20 21 22 23 24 25 26 27 28 **2. Materials and Methods**

29  
30  
31 The chemicals, cadmium oxide CdO, oleic acid, octadecene, selenium powder, trioctylphosphine  
32 (TOP) and mercaptopropionic acid (MPA), were bought from Sigma-Aldrich and were used as  
33 received. Deionized water from Organo Biotech Laboratories, India, was used to prepare the  
34 solutions. CdSe quantum dots (QDs) were synthesized from CdO and elemental Se using a  
35 kinetic growth method pioneered by Peng and others.<sup>19-28</sup> This approach has several advantages  
36 relative to conventional CdSe QD synthesis methods.<sup>29</sup> In particular, the typical precursor  
37 material, especially dimethyl cadmium, is extremely toxic, expensive, unstable, explosive, or  
38 pyrophoric in nature, making the system difficult to handle.<sup>22, 29</sup> Although the hazards associated  
39 with the CdO and Se should not be overlooked, the kinetic synthesis method we employ is  
40 viewed as an example of green chemistry with improved safety and reduced toxicity.

41  
42  
43 A stock solution of Se precursor was prepared ahead of time by combining 30 mg of Se  
44 and 5 mL of 1-octadecene (ODE) in a 10-mL round-bottom flask clamped over a hot plate. A  
45 syringe was used to measure 0.4 mL of trioctylphosphine from its Sure-Seal bottle and added to  
46 the same flask, and the solution was stirred. It was warmed to facilitate speedy dissolution of the  
47 Se. The stock solution was stored at room temperature (25 °C) in a sealed container, and had  
48 enough Se precursors for five preparations.

1  
2  
3  
4  
5  
6  
7  
8  
9  
10  
11  
12  
13  
14  
15  
16  
17  
18  
19  
20  
21  
22  
23  
24  
25  
26  
27  
28  
29  
30  
31  
32  
33  
34  
35  
36  
37  
38  
39  
40  
41  
42  
43  
44  
45  
46  
47  
48  
49  
50  
51  
52  
53  
54  
55  
56  
57  
58  
59  
60

Cd precursor was prepared by adding 13 mg of CdO to a 25-mL round-bottom flask clamped on a heating mantle. To the same flask 0.6 mL of oleic acid and 10 mL of octadecene were added and the flask was heated. When the temperature reached 225 °C, 1 mL of the room-temperature selenium solution was transferred to the hot cadmium solution. Because the physical characteristic of the nanoparticles strongly depends on reaction time, timing began when the selenium solution was added. A 2 mL disposable syringe was used to remove and quench approximately 1 mL samples at specific time intervals, as quickly as possible at the beginning of the synthesis and at later times when noticeable color change was detected.

Colloidal CdSe QDs prepared in TOP ( trioctylphosphine/dodecylamine) were transferred into water medium by the use of amino-ethanethiol. HCl (AET) or mercaptopropionic acid (MPA).<sup>30,31</sup> To prepare CdSe QDs with a negatively charged MPA capping, 100 µL of the crude solution of CdSe QDs in the TOP coordinating mixture was dissolved in 5 mL of chloroform. Subsequently, a 0.5 M methanolic solution of MPA-KOH (with 20 mol % excess of KOH) was added until the particles flocculated. Directly after the flocculation, ultrapure water was added to the suspension, resulting in a two-phase system (water above chloroform). Upon shaking, the QDs were transferred into the water phase. The KOH solution was added to the MPA solution in order to deprotonate the carboxylic groups of MPA. No post-preparative steps were required to clean up the CdSe QDs solution, since TOP stay in the chloroform phase rather than in the water phase. The pH of CdSe quantum dot dispersion was ~ 9.0±0.5.

UV-Vis absorption spectra were obtained using spectrophotometer (Model CE-7300, Cecil Instruments, U. K.) operating in the wavelength range from 190 to 900 nm. FTIR spectra from all samples were recorded on a FT-IR/ Raman Spectrometer (1064 nm) attached to a microscope (Varian 7000 FT-Raman and Varian 600 UMA). We adopted FT-IR Spectroscopy to investigate structure of water in various solutions because vibrational spectra are very sensitive to the local molecular environment. Average particle sizing was done by using a JEOL 2100F, TEM (Digital TEM with image analysis system at a maximum magnification of 1, 50,000X operating at a voltage 200 kV). The dispersion state particle sizing was also done by dynamic light scattering (DLS) technique. The instrument used for this purpose is described elsewhere.<sup>32</sup> Further details about the principle of operation of the DLS instrument and data analysis of correlation function can be obtained from ref.<sup>33</sup>.

The steady state fluorescence measurements were performed using Varian Cary Eclipse fluorescence spectrophotometer having spectral range from 190 to 1000 nm, and lifetime decay experiments were performed using time-correlated single photon counting (TCSPC) setup (FL920, Edinburgh Instrument). All samples were excited with diode lasers and the emission decays were collected at emission peak wavelength at magic angle polarization ( $55^{\circ}$ ). Here, we have used pico-second time resolved fluorescence spectrometer (TRFS) to probe the solvent effect on the lifetime of relaxations. All the measurements were performed with 100 nm TAC (Time to Amplitude Converter) at excitation wavelengths of 375 and 405 nm LED source. The time resolution for TCSPC setup was  $\sim 120$  ps (measured with LUDOX solution). The decay curves were least-squares fitted to the single-exponential decay function given by

$$F(t) = a_0 + a_1 \exp\left(-\frac{t}{\tau}\right) \quad (1)$$

where  $a_0$  defines the time shift between instrument response function, and the sample. The mean relaxation time  $\tau$  corresponds to the average lifetime of characteristic excited states. The goodness-of-fit  $\chi^2$  chi-square parameter obtained was greater than 99 % indicating robust and reproducible least square fitting of the data.

### 2.1 Preparation of bacterial culture

The bacterial cultures (*E. coli-DH5 $\alpha$* , Gram-negative bacteria) and (*S. aureus*, Gram-positive bacteria) were maintained in nutrient agar at 37°C. Bacterial inoculations were prepared to 0.5 McFarland standards before performing the antimicrobial assays. Briefly, the primary inoculation was performed in nutrient broth at 37 °C and was kept overnight at 180 rpm in the shaker incubator. Secondary inoculation was also done and the flask was incubated at 37 °C for 4h. The turbidity of the resulting suspension was observed and optical density (O.D) was measured at 600 nm using UV spectrophotometer (Agilent Technology, Germany). These bacterial cultures were used for further experiments.

### Toxicity assessment

#### 2.2 Bactericidal assay

Bacteriocidal activity by disc diffusion assay (Kirbey-Bauer method) against *E. coli* and *S. aureus* was performed as per previously published protocol<sup>34,35</sup>. Briefly, hard agar using Luria

1  
2  
3 agar (3.5 %) and Agar agar (0.8 %) were prepared and autoclaved. After cooling, the hard agar  
4 was poured onto the petri-plates and was allowed to solidify. Agar agar containing bacterial  
5 inoculum was prepared. This was evenly poured on the previously prepared solidified agar  
6 plates. 20  $\mu\text{L}$  of QDs were impregnated onto 3 mm sterile blank discs and allowed to dry before  
7 placing onto the culture plates on the marked areas. Plates inoculated with bacteria were  
8 incubated overnight at 37 °C. Bacteriocidal activity was directly proportional to the diameter of  
9 inhibition zone. Gentamycin sulphate ( $1 \times 10^{-3}$   $\mu\text{g}/\text{ml}$ ) was used as positive control.

### 16 **2.3 Cytotoxicity assessment**

17 Percentage reduction in cellular viability after the interaction period (24 h) was determined using  
18 MTT assay as described by Mossman<sup>36</sup>. In the recent past, the MTT assay has been employed as  
19 a method for analyzing cellular viability of prokaryotes<sup>37</sup>. Interference shown by QDs with MTT  
20 dye was subtracted from the results. The increase in bacterial cytotoxicity in treated samples was  
21 calculated with respect to control. Cell culturability was determined using standard plate count  
22 assay on LB agar medium. EC50 value was calculated by MTT assay.

### 30 **Exposure of bacterial cultures to QDs**

31 *S. aureus* and *E. coli* ( $5 \times 10^9$  cells; concentrated 5 ml culture) were treated with QDs at 37 °C for  
32 24 h.

### 35 **Oxidative stress markers**

#### 37 **2.4 Lactate dehydrogenase (LDH) release/membrane integrity**

38 Membrane integrity of the treated culture was assessed by extracellular LDH release assay. Data  
39 were reported as percentage release of LDH compared to control LDH release. The level of  
40 extracellular LDH release was assessed as an indicator of membrane permeability and  
41 cytotoxicity. As per the protocol by Kumar A. et al. 2011<sup>38</sup>, the interacted bacterial cell  
42 suspension was centrifuged (7000g, 10 min), and the LDH level in the supernatant was measured  
43 following the standard protocol. To 100  $\mu\text{L}$  of supernatant, 100  $\mu\text{L}$  of 30 mM sodium pyruvate  
44 and 2.8 mL of 0.2 M Tris-HCl was added. One hundred microliters of 6.6 mM NADH were  
45 added prior to use. The rate of decrease in absorbance at 340 nm in a 96-well plate using a (KC4)  
46 Synergy HT multiwell plate reader (Bio-Tek) to determine the LDH release activity.

## 2.5 Determination of reactive oxygen species (ROS)

Intracellular ROS in the bacterial cells were measured using dichlorofluorescein diacetate (DCFH-DA) as described by Lyon et al.<sup>39</sup> with minor modifications. Bacterial culture (1 ml) was pelleted by centrifugation at 5000g for 5 min. The pellet was resuspended in PBS containing 30 µg/ml DCFHDA dye at 37 °C for 30 min in shaker. Further, the treated culture was pelleted and resuspended in 450 µl of PBS, and fluorescence values were measured at an excitation wavelength of 485 nm and emission wavelength of 528 nm in a 96-well plate using a (KC4) Synergy HT multiwell plate reader (Bio-Tek).

## 2.6 Glutathione levels

Reduced glutathione levels were estimated by method previously described by Scott et al.<sup>40</sup>, with slight modification. Bacteria were cultured to  $1 \times 10^9$  cfu/ml and treated with QDs. An aliquot of 1ml was extracted with 50 µl of 100% TCA. The mixture was kept in ice for 10 min and centrifuged at 10,000g for 5 min. After precipitation, 200 µl of 30 mM Tris-HCl (pH 8.9) buffer was used to neutralize the sample. Further, GSH was quantified by measuring absorbance at 412 nm by reaction between 500 µl of supernatant and 2.5 ml of 0.01% dithionitrobenzoate after incubation for 15–20 min; simultaneously, a 0.4 ml portion of the remaining treated culture was used for determination of protein using the Bradford method. Glutathione levels were estimated after normalization to cellular protein levels and expressed as GSH µmol/mg protein.

## 2.7 DNA fragmentation

DNA fragmentation was measured using the DPA assay. The DNA from the QD-treated bacteria was isolated using the described protocol. The diphenylamine (DPA) reaction was performed according to the method described by Paradones *et al.* and Sally *et al.*<sup>41,42</sup>. Perchloric acid (0.5 M) was added to the cell pellets containing uncut DNA (resuspended in 200 µL of hypotonic lysis buffer) and to the other half of the supernatant containing DNA fragments. Then two volumes of a solution consisting of 0.088 M DPA, 98% (v/v) glacial acetic acid, 1.5% (v/v) sulphuric acid, and a 0.5% (v/v) concentration of 1.6% acetaldehyde solution were added. The samples were stored at 4°C for 48 h. The reaction was quantified spectrophotometrically at 575 nm. The percentage of fragmentation was calculated as the ratio of DNA in the supernatants to the total DNA.

### 3. Results and Discussion

#### 3.1 Characterization of CdSe quantum dots

Fig. 1(a) depicts the photographs of QDs taken in normal light and under UV illumination which clearly indicate the fluorescent property of these nanoparticles. A representative TEM image is shown Fig. 1(b). DLS study indicated that the mean hydrodynamic diameter of these particles was  $6.8 \pm 0.4$  nm. In comparison, TEM analysis revealed the presence of nearly monodisperse particles having average diameter of  $6.5 \pm 0.4$  nm. The observed difference in the two sizes was remarkably small regardless of the fact that TEM data corresponded to dehydrated samples. Therefore, we concluded that the average particle size observed from TEM was more likely to represent the actual size of QDs whereas DLS result referred to the size of hydrated particles. The size of the QDs can be controlled by regulating the nucleation temperature and the growth time, but not continuously. By this method, we could prepare QDs of three distinct sizes only (2.43, 3.75 and 5.09 nm).

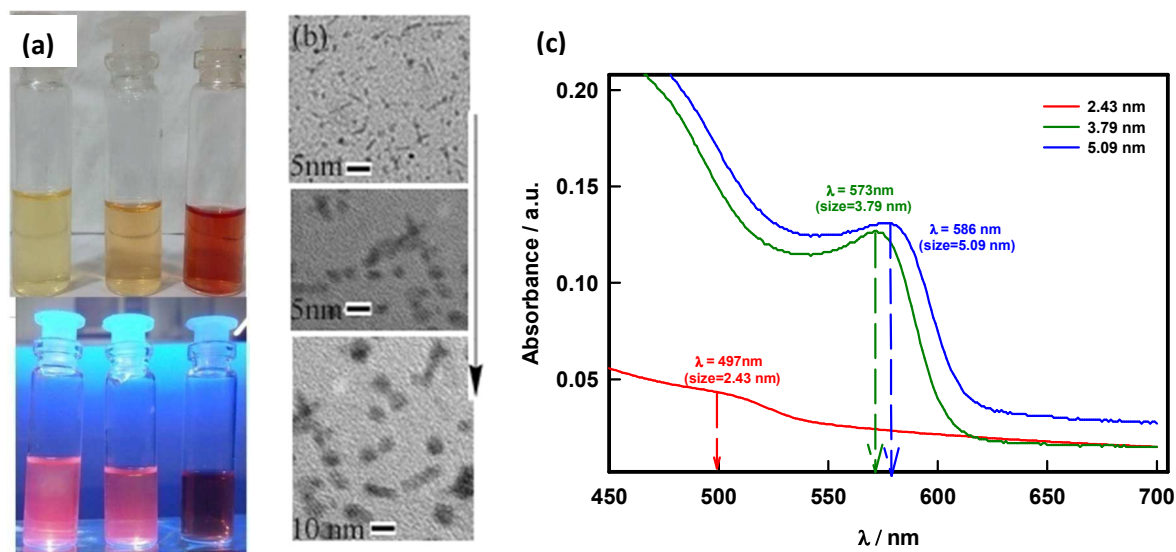


**Fig. 1.** (a) Photographs (normal light (top left) and UV-illumination (bottom right)) and (b) TEM image (middle) and (c) UV-vis absorption spectra of water soluble CdSe QDs (right).

Fig. 1(c) depicts the UV-vis absorption spectra of QD samples. The absorption edge of the curves showed a clear blue-shift from bulk band gap, indicating the quantum nature of the nanoparticles. A well-resolved absorption maximum of the first electronic transition was observed that attributed a narrow size distribution to these preparations. The particle diameters  $D$

of QDs were determined from the first absorption maximum of the UV–vis absorption spectra according to the following empirical formula given by

$$D(\text{nm}) = 59.60816 - 0.54736\lambda + 1.8873 \times 10^{-3}\lambda^2 - 2.85743 \times 10^{-6}\lambda^3 + 1.62974 \times 10^{-9}\lambda^4 \quad (3)$$

where D (nm) is the diameter of a given QD particle, and  $\lambda$  (nm) is the wavelength of the first excitonic absorption peak of the concerned sample. The diameter values are listed in Table-I.

Results showed that the particle diameters of the as prepared CdSe QDs were about 2.43, 3.75 and 5.09 nm corresponding to the first absorption maximum of 497, 573 and 586 nm respectively. The concentrations of the CdSe dispersions were determined from the UV-Vis data using Beer-Lambert's law. Zeta potential ( $\zeta$ ) of these nanoparticles were measured using electrophoresis instrument (Zeecom–2000, Microtek, Japan) from which, in principle, one could determine the surface charge on these particles if their morphologies are known. The particle size, and their distribution were determined using dynamic light scattering (DLS), and transmission electron microscopy (TEM) techniques. These results are listed in Table 1.

Table 1: Physical characteristics of the samples used in this study measured at room temperature 20 °C. Sizes reported are mean values.

Sample ID	DLS size/nm	TEM size/nm	UV-vis size/nm	pH	Zeta potential/mV	Fluorescence lifetime/ns
A	3.8±0.2	3.5±0.2	2.43±0.08	9.0±0.5	-50±2	0.010±0.001
B	4.9±0.3	4.7±0.3	3.75±0.09	9.0±0.5	-56±3	0.011±0.001
C	6.8±0.4	6.5±0.4	5.09±0.07	9.0±0.5	-60±3	0.013±0.001

### 3.2 Steady state and Time Resolve Fluorescence spectroscopy

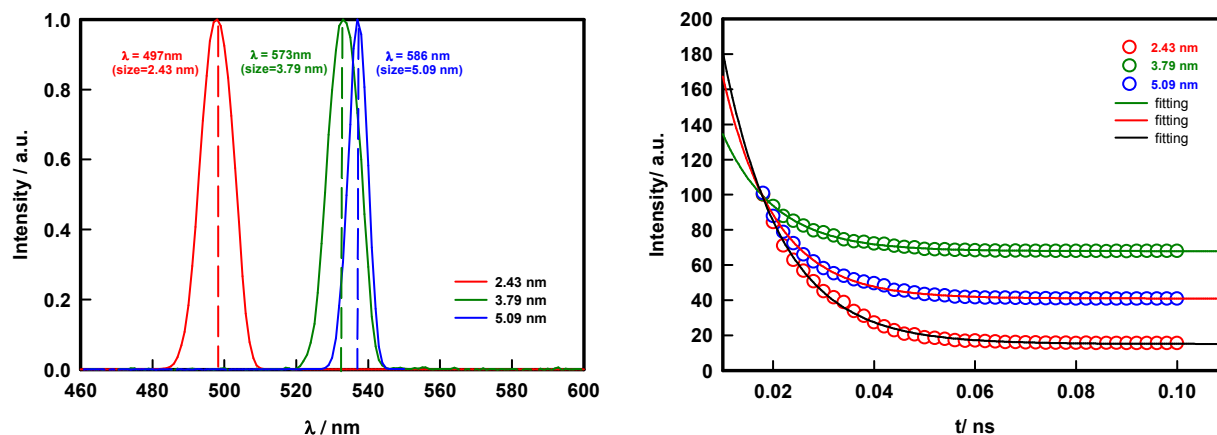


**Fig. 2.** (a) Steady state (left) and (b) time resolved fluorescence spectra of QD samples of different size recorded at room temperature(right).

Size dependent fluorescence of QDs was probed using steady state fluorescence spectroscopy where we observed a red-shift in the emission maxima with size (Fig. 2a). The aqueous dispersion of MPA capped CdSe quantum dots with increasing size of solution and the fluorescence intensity was monitored as shown in Fig. 2(a).

Fluorescence emission decay spectra reported herein were obtained from TCSPC experiments. A 405 nm LED source was used to excite the samples, and record the time decay signal at the emission maximum of 350 nm. These time resolved fluorescence decay curves are depicted in Fig. 2(b), and these curves were fitted to exponential decay function given by eq (1). The exciton lifetime had minor dependence on size of QDs (Table 1). The decay time progressively decreased with increase in the size of QD. And the decrease was close to 30%.

### 3.3 Antimicrobial activity

The results of the antimicrobial activities of quantum dots using disc diffusion assay is represented in (Fig.3 and Table 2)

These inorganic QDs offer distinct advantages over chemical based antimicrobial agents that are known to cause time-dependent multidrug resistance. The membrane structure of gram-positive and gram-negative bacteria has been differentiated based on the thickness of the peptido-glycan layer that is a distinct feature of the prokaryotes. The lower efficacy of the QDs against *S. aureus* may possibly be due to the difference in the membrane structure. To further

endorse this premise, more differential study between gram-negative and gram-positive bacterial species was required.

*Staphylococcus aureus* (gram positive), in sample A (2.43 nm), indicated the highest inhibition zone of 3.5 mm, sample B (3.75 nm) showed slight inhibition zone of 1.25 mm. However, in sample C (5.09 nm) 2.75 mm zone of inhibition was observed. In case of *Escherichia coli* DH5 $\alpha$  (gram negative), sample A (2.43 nm), the highest inhibition zone of 5 mm was observed on the agar disc assay. Moreover, sample B (3.75 nm) indicated an inhibition zone of 2 mm. However, in sample C (5.09 nm) a 4 mm zone of inhibition was observed. Gentamycin was used as the positive control ( $1 \times 10^{-3}$   $\mu\text{g/ml}$ ) and Distilled water was used as negative control. All the QD-stock samples have 20 mg/mL concentration.

Table 2: Antibacterial activity of QDs on *E. coli* and *S. aureus*. Zone of inhibition reported are mean  $\pm$  S.D values.

S. No.	Samples (size)	Positive control (mm)		Negative control (mm)	Zone of Inhibition (mm)	
		<i>S. aureus</i>	<i>E. coli</i> DH5 $\alpha$		<i>S aureus</i>	<i>E. coli</i> DH5 $\alpha$
1.	A (2.43 nm)	6.75 $\pm$ 0.09	2.5 $\pm$ 0.11	-	3.50 $\pm$ 0.10***	0.5 $\pm$ 0.10***
2.	B (3.75 nm)	6.75 $\pm$ 0.12	2.5 $\pm$ 0.21	-	1.25 $\pm$ 0.20***	0.2 $\pm$ 0.07***
3.	C (5.09 nm)	6.75 $\pm$ 0.15	2.5 $\pm$ 0.11	-	2.75 $\pm$ 0.15***	0.4 $\pm$ 0.15***

\*indicates significance difference between control and treated groups. One way ANOVA was performed followed by Tukey's test. Asterisks indicate levels of significance. \*\*\* $p < 0.001$ , \*\* $p \leq 0.01$ , \* $p \leq 0.05$

### 3.4 Cell viability assessment

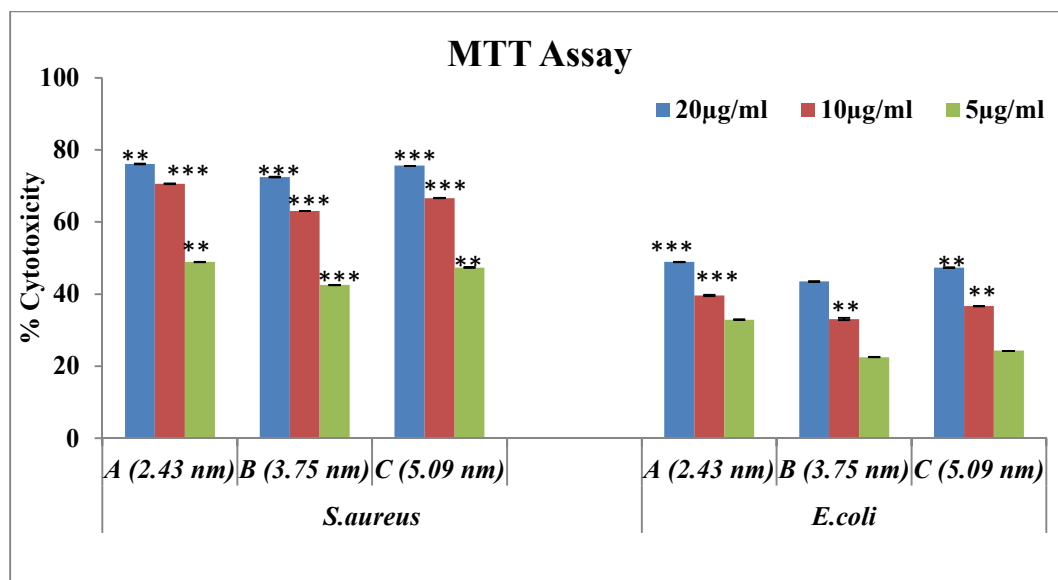


Fig 3: Cell viability assessment in *S. aureus* and *E. coli* (24 h) by MTT assay. Data are reported as mean  $\pm$  SD from three independent experiments; \*\*\* $p < 0.001$ , \*\* $p \leq 0.01$ , treated groups compared with control.

Concentration dependent reduction in cell viability of *S. aureus* and *E. coli* upon QDs incubation was observed by MTT assay. MTT assay showed a significant increase in cytotoxicity in both gram-positive and gram-negative bacteria, *S. aureus* and *E. coli* [QD A (2.43 nm,  $70.61 \pm 0.093\%$  and  $39.61 \pm 0.049\%$ ) and C (5.09 nm,  $66.65 \pm 0.022\%$  and  $36.65\% \pm 0.104\%$ ) followed by B (3.75 nm,  $63.08 \pm 0.104\%$  and  $33.08\% \pm 0.043\%$ )], as compared to control, at  $10 \mu\text{g mL}^{-1}$  concentration (Fig. 3). At these concentrations, the difference in cytotoxicity under conditions was found to be significant. One-way ANOVA followed by Tukey's test was performed to calculate the statistical significance in values. EC<sub>50</sub> values of QD A (2.43 nm), B (3.75 nm), C (5.09 nm) were calculated by MTT assay varied significantly for *S. aureus* ( $5.154 \mu\text{g/ml}$ ,  $5.882 \mu\text{g/ml}$  and  $5.279 \mu\text{g/ml}$ ) and *E. coli* ( $20.448 \mu\text{g/ml}$ ,  $22.985 \mu\text{g/ml}$  and  $21.119 \mu\text{g/ml}$ ).

### 3.5 Effects of QDs on LDH release and membrane integrity

LDH is an important marker for oxidative stress induced cell death. The effects of QDs on LDH release of *S. aureus* and *E. coli* cells are indicated in Fig. 4. Bacterial cells exposed to QDs demonstrated a size dependent release of LDH (Fig. 4). A significant release of LDH was observed after 24 h exposure to the QDs showing an increase in membrane permeability. QDs A and C induced release of LDH compared to the control group, and a slight decrease in QD-B

(3.75 nm) [LDH level by QD A (2.43 nm, 104.05%  $\pm$  5.77% and 102.61%  $\pm$  13.76%) and C (5.09 nm, 68.89%  $\pm$  7.21% and 29.4%  $\pm$  15.12%) followed by B (3.75 nm, 51.68%  $\pm$  11.54% and 18.45%  $\pm$  15.46%)]. Interestingly, some differences between Gram positive *S. aureus* and Gram negative *E. coli* were observed.

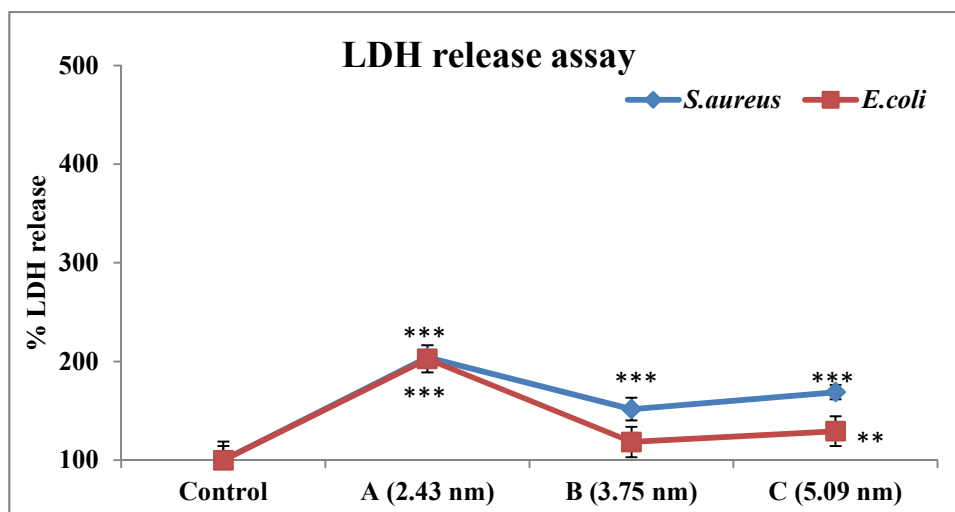


Fig 4. Assessment of membrane damage (24 h) by LDH release assay. The cells were exposed to 20 $\mu$ l QDs for 24 h. Each plot was produced from at least 3 replicate measurements. All values are presented as mean  $\pm$  S.D. ( $n \geq 3$ ). All the QD-stock samples have 20 mg/mL concentration.

\*indicates significance difference between control and treated groups. One way ANOVA was performed followed by Tukey's test. Asterisks indicate levels of significance. \*\*\* $p < 0.001$ , \*\* $p \leq 0.01$ , \* $p \leq 0.05$

### 3.6 Reduced glutathione assay (GSH)

In the past few years, there has been increasing interest in the measurement of thiols, glutathione as indicators of oxidative stress. The reduced glutathione/oxidized glutathione ratio (GSH/GSSG) was used to evaluate the oxidative stress status in biological systems, and alterations of this ratio have been demonstrated in cancer and other diseases.<sup>43</sup> The decrease in the reduced glutathione content might reflect decreased levels of the activity of glutathione reductase in *S. aureus* and *E. coli* [GSH level in *S. aureus* and *E. coli* by QD A (2.43 nm=0.055  $\pm$  0.0007, 0.053  $\pm$  0.0002), C (5.09 nm=0.057  $\pm$  0.001, 0.054  $\pm$  0.0046) followed by B (3.75 nm=0.060  $\pm$  0.0003, 0.057  $\pm$  0.0005) in comparison to control (0.086  $\pm$  0.001, 0.075  $\pm$  0.0005)]. Consistent with our results, earlier it has been suggested that QDs treatment in *S. aureus* and

*E. coli* leads to enhanced levels of reactive oxygen intermediates with reduced content of glutathione.<sup>44</sup> The level of reduced glutathione was observed to deplete significantly in interacted bacterial cells compared to control (Fig.5). The GSH level in *S. aureus* and *E. coli* was found to be relatively less in QD A (2.43 nm=0.055 ± 0.0007, 0.053 ± 0.0002) compared to C (5.09 nm=0.057 ± 0.001, 0.054 ± 0.0046) followed by B (3.75 nm=0.060 ± 0.0003, 0.057 ± 0.0005) in both the bacterial strains. Cellular GSH levels were significantly depleted after 24 h exposure to QD-A followed by QD-C and then by QD-B respectively, compared to control (0.086 ± 0.001, 0.075 ± 0.0005).

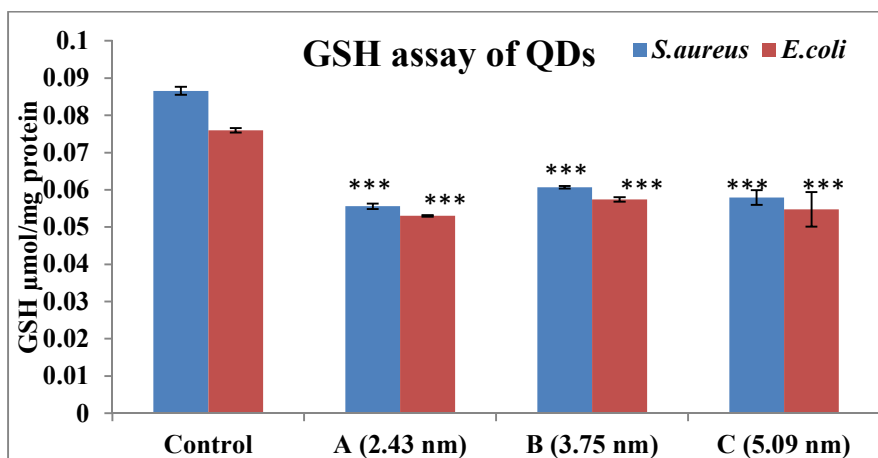


Fig 5. Reduced glutathione (GSH) levels in QDs exposed bacterial cells. The cells were exposed to 20µl QDs for 24 h. Each plot was produced from at least 3 replicate measurements. All values are presented as mean ± S.D. (n ≥3). All the QD-stock samples have 20 mg/mL concentration.

### 3.7 Determination of intracellular reactive oxygen species (ROS)

QD-A showed a significant size dependent increase (2.43 nm) in intracellular ROS generation when compared to control (Fig.6). Though both QDs A and C showed ROS induction in *S. aureus* and *E. coli*, it was more pronounced in *S. aureus* than *E. coli*. The QDs of 2.43 nm are most likely to get entangled in the teichoic acid and lipopolysaccharide. The QDs of 5.09 nm are much larger than the bacterial pores and were internalized only when a perturbation occurs in the cell membrane. 3.75 nm sized QDs appeared to be optimal sized, as they could penetrate the cell walls. Small sized QDs had a better mobility than the larger QDs and were therefore had a better chance to contact cells and further caused a higher extent of cytotoxicity. The correlation between size and cytotoxicity was observed with CdTe QDs. Lovrić et al. (2005)<sup>45</sup> observed

that the green fluorescence CdTe QDs (2.2±0.1 nm in diameter) exhibited higher cytotoxic effects than the red fluorescence QDs (5.2±0.1 nm in diameter), our findings confirmed that QDs were internalized by bacterial cells and induced significant oxidative stress [QD-A (119.35% ± 5.77 % and 34.58% ± 5.77%) > QD-C (62.90% ± 11.54% and 23.3% ± 5.77%) > QD-B (14.51% ± 15.27% and 12.03% ± 5.77%)]. (Fig. 6)

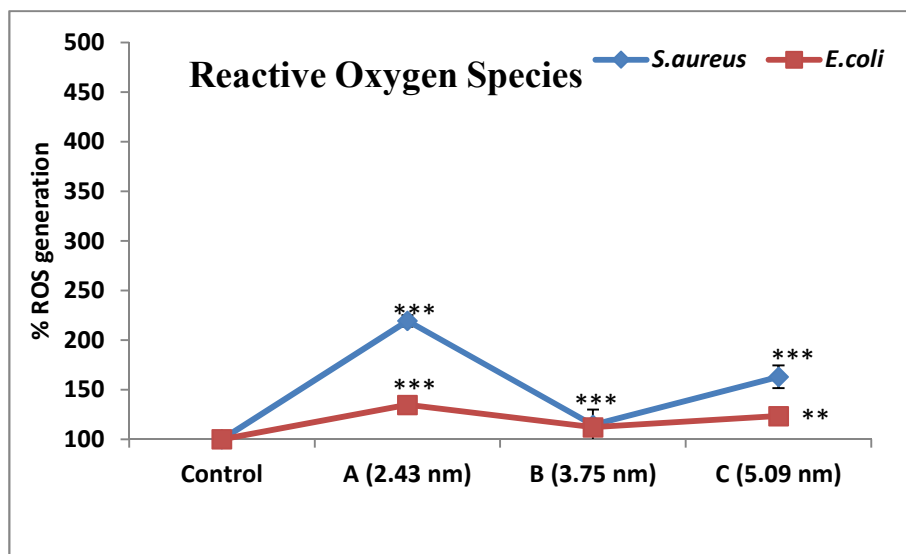


Fig.6 Reactive oxygen species (ROS) generation in QDs exposed bacterial cells. The cells were exposed to 20µl QDs for 24 h. Each plot was produced from at least 3 replicate measurements. All values are presented as mean ± S.D. (n ≥3). All the QD-stock samples have 20 mg/mL concentration.

### 3.8 DNA fragmentation assay

The molecular mechanism of cell death has further been assessed by DNA fragmentation analysis using DPA assay (Fig.7) where the percentage of DNA fragmentation by different sized QDs clearly indicated significant DNA damage in both *S. aureus* (QD-A>QD-C>QD-B = 53% ± 1.5%, 49% ± 1.15% , 47% ± 1.15%) and *E. coli* (49.5% ± 1.73% , 45% ± 0.57% , 42% ± 1.15%). Thus, our study reveals details of death process induced by QDs. Based on these observations, a hypothetical mechanism for cellular toxicity could be proposed by the generation of OH<sup>•</sup>, O<sup>2-</sup>, and H<sub>2</sub>O<sub>2</sub> in bacterial cells leading to oxidation of polyunsaturated phospholipids. Production of singlet oxygen [O] has been recognized as the cause of oxidative stress<sup>46</sup>. The intracellular ROS subsequently causes DNA damage, GSH depletion, and

disruption of membrane morphology that eventually leads to cell death.<sup>47,48</sup> Increase in the free radicals changes results in phenomenal alternations in the DNA, thereby pushing the cell into apoptosis evidenced by percent DNA fragmentation.

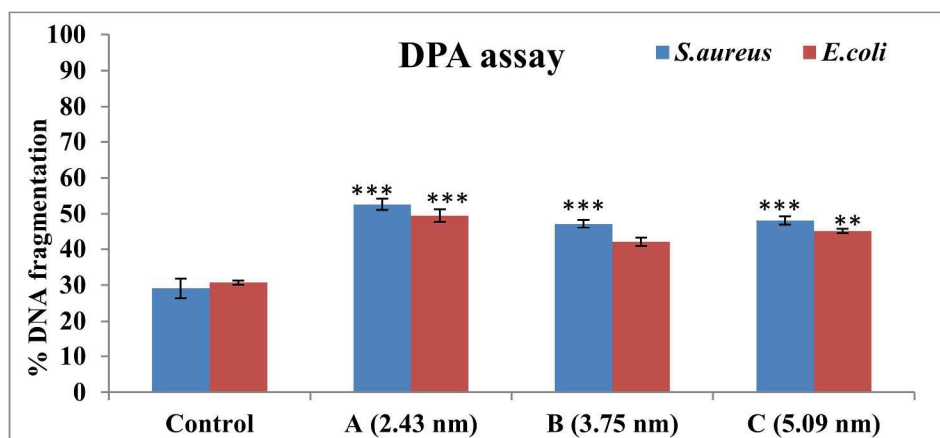


Fig 7. Quantification of DNA fragmentation for *S. aureus* and *E. coli* using DPA assay in the control and experimental groups. Bars are mean  $\pm$  S.D. Values in the parenthesis are percent change from that of control. All the QD-stock samples have 20 mg/mL concentration.

### 3.9 Statistical Analysis

The results were expressed as mean  $\pm$  SD. Comparison between control and treated groups were analyzed by One-way ANOVA followed by Tukey's test using Prism (5.0) software (Prism software Inc.CA). \*indicates significance difference between control and treated groups. A p-value of  $<0.05$  was considered significant.

### Conclusions

We have reported synthesis of CdSe quantum dots by hot injection method and the fluorescent QDs were probed for their luminescent signature. The fluorescent lifetime increased with QDs size. *In vitro* results indicated that the antibacterial activity of small sized QDs Sample A (2.43 nm) was significantly enhanced. The sensitivity of *S. aureus* was higher in all the different sized QDs when compared to *E. coli*. This question about size dependent toxicity issue came to our mind while doing the experiments, particularly when we were comparing the bactericidal activity

1  
2  
3 of the QDs. This paper includes only the antimicrobial assessment of the QD activity.  
4 Comparison with the in vitro results has not been included in this work. The in vitro results  
5 indicated that the antibacterial activity of smallest size QD Sample A (2.43 nm) was significantly  
6 higher which is in consistence with known literature.  
7  
8

9  
10 Further mechanistic studies on the toxic response to QDs revealed that LDH release was  
11 inversely proportional to the reduced glutathione content (GSH) of the organism. The oxidative  
12 stress induced by QDs post internalization causes the membrane leakage, as well as the DNA  
13 fragmentation in the cell. These observations reflect the possible perturbations that could  
14 possibly inflict damage to many unwanted members of microbial communities responsible for  
15 biogeochemical cycles in aquatic and terrestrial environment. Our observations substantiate the  
16 need for impact assessment of such novel materials in environmental settings.  
17  
18  
19  
20  
21  
22  
23  
24

## 25 **Acknowledgment**

26  
27  
28 We are thankful to Advanced Research Instrumentation Facility of the University for allowing us  
29 access to TRFS facility. AT is thankful to UGC for her JRF. KR acknowledges receipt of DST-  
30 Inspire Faculty award from Department of Science and Technology, Government of India.  
31  
32  
33  
34  
35  
36

## 37 **Declaration**

38  
39 Authors declare no financial competing interest.  
40  
41

## 42 **Reference**

- 43  
44 1. V. Biju, A. Anas, T. Itoh, A. Sujith and M. Ishikawa, Semiconductor quantum dots and  
45 metal nanoparticles: Syntheses, optical properties, and biological applications. *Analytical*  
46 *and Bioanalytical Chemistry*, 2008, **391**, 2469 – 2495.
- 47  
48 2. A. P. Alivisatos, Semiconductor Clusters, Nanocrystals, and Quantum Dots. *Science*  
49 1996, **271**, 933–937.
- 50  
51 3. 3. Vanmaekelbergh D, Liljeroth P: Electron-conducting quantum dot solids: novel  
52 materials based on colloidal semiconductor nanocrystals. *Chem Soc Rev* 2005, 34:299-  
53 312.  
54  
55  
56  
57  
58  
59  
60

- 1  
2  
3  
4 4. Pathak S, Cao E, Davidson MC, Jin SH, Silva GA: Quantum dot applications to  
5 neuroscience: New tools for probing neurons and glia. *Journal of Neuroscience* 2006,  
6 26:1893-1895.
- 7  
8  
9 5. Yu WW, Qu LH, Guo WZ, Peng XG: Experimental determination of the extinction  
10 coefficient of CdTe, CdSe, and CdS nanocrystals. *Chem Mater* 2003, 15:2854-2860.
- 11  
12 6. Osaki F, Kanamori T, Sando S, Sera T, Aoyama Y: A Quantum Dot Conjugated Sugar  
13 Ball and Its Cellular Uptake. On the Size Effects of Endocytosis in the Subviral Region.  
14 *JACS* 2004, 126:6520-6521.
- 15  
16  
17 7. W.W. Yu, E. Chang, R. Drezek and V. L. Colvin, Interactions Of Biotinylated Viral  
18 Oligonucleotides With Streptavidin - Modified Quantum Dots Studied By Capillary  
19 Electrophoresis. *Biochemical and Biophysical Research Communications* 2006, **348**,  
20 781–786.
- 21  
22  
23 8. S. Sanwani, K. Rawat, M. Pal, H. B. Bohidar and A. K. Verma, Cellular Uptake induced  
24 biotoxicity of Surface Modified CdSe Quantum Dots. *J. Nanopart. Res.*, 2014, **16**, 2382-  
25 1-11.
- 26  
27  
28 9. W. C. W. Chan, D. J. Maxwell, X. Gao, R. E. Bailey, M. Han and S. Nie, Luminescent  
29 quantum dots for multiplexed biological detection and imaging. *Current Opinion in*  
30 *Biotechnology*, 2002, **13**, 40–46.
- 31  
32  
33 10. W. W. Yu, E. Chang, J. C. Falkner, J. Zhang, A. M. Al-Somali, C. M. Sayes, J. Johns, R.  
34 Drezek and V. L. Colvin, Forming biocompatible and nonaggregated nanocrystals in  
35 water using amphiphilic polymers. *J. Am. Chem. Soc.* 2007, **129**, 2871–2879.
- 36  
37  
38 11. H. T. Uyeda, I. L. Medintz, J. K. Jaiswal, S. M. Simon and H. Mattoussi, Synthesis of  
39 Compact Multidentate Ligands to Prepare Stable Hydrophilic Quantum Dot  
40 Fluorophores. *J. Am. Chem. Soc.* 2005, **127**, 3870–3878.
- 41  
42  
43 12. D. J. Norris, A. Sacra, C. B. Murray and M. G. Bawendi, Measurement of the size  
44 dependent hole spectrum in CdSe quantum dots. *Physical Review Letters* 1994, **72**,  
45 2612–2615.
- 46  
47  
48 13. M. A. Hines and P. Guyot-Sionnest, Synthesis and characterization of strongly  
49 luminescing ZnS-capped CdSe nanocrystals. *Journal of Physical Chemistry* 1996, **100**,  
50 468–471.
- 51  
52  
53  
54  
55  
56  
57  
58  
59  
60

14. J. Adana, Y. A. Wang and X. Peng, Photochemical Instability of CdSe Nanocrystals Coated by Hydrophilic Thiols. *J. Am. Chem. Soc.* 2001, **123**, 8844-8850.
15. S. Sadhu, P. S. Chowdhury and A. Patra, Synthesis and time-resolved photoluminescence spectroscopy of capped CdS nanocrystals. *J. Lumin.* 2008, **128**, 1235-1240.
16. N. Gaponik, I. L. Radtchenko, G. B. Sukhorukov, H. Weller and A. L. Rogach, Toward Encoding Combinatorial Libraries: Charge-Driven Microencapsulation of Semiconductor Nanocrystals Luminescing in the Visible and Near IR. *Adv. Mater* 2002, **14**,879–882.
17. D. V. Talapin, A. L. Rogach, E. V. Shevchenko, A. Komowski, M. Haase and H. Weller, Dynamic Distribution of Growth Rates within the Ensembles of Colloidal II-VI and III-V Semiconductor Nanocrystals as a Factor Governing their Photoluminescence Efficiency. *J. Am. Chem. Soc.* 2002, **124**, 5782–5790.
18. L. Peng, M. He, B. Chen, Q. Wu, Z. Zhang, D. Pang, Y. Zhu, B. Hu, Cellular uptake, elimination and toxicity of CdSe/ZnS quantum dots in HepG2 cells, *Biomaterials*, 2013, **34**(37), 9545–9558.
19. A. C. S. Samia, X. Chen and C. Burda, Semiconductor Quantum Dots for Photodynamic Therapy. *J. Am. Chem. Soc.* 2003, **125**, 15736–15737.
20. A. C. S. Samia S. Dayal and C. Burda, Quantum Dot Based Energy Transfer: Perspectives and Potential Applications in Photodynamic Therapy," *Photochem. Photobiol. Photochem. Photobiol.* 2006, **82**, 617–625.
21. Z. A. Peng and X. Peng, Nearly monodisperse and shape-controlled CdSe nanocrystals via alternative routes: Nucleation and growth. *J. Am. Chem. Soc.* 2002, **124**, 3343–3353.
22. Z. A. Peng and X. Peng, Formation of High-Quality CdTe, CdSe, and CdS Nanocrystals Using CdO as Precursor. *J. Am. Chem. Soc.* 2001, **123**, 183–184.
23. X. Peng, Approaches toward High-Quality Semiconductor Nanocrystals. *Chem. Eur. J.* 2002, **8**, 335–339.
24. L. Qu, A. Peng and X. Peng, Alternative Routes toward High Quality CdSe Nanocrystals. *Nano Letters* 2001, **1**, 333–337.
25. L. Qu, and X. Peng, Control of Photoluminescence Properties of CdSe Nanocrystals in Growth. *J. Am. Chem. Soc.* 2002, **124**, 2049-2055.

- 1  
2  
3  
4  
5  
6  
7  
8  
9  
10  
11  
12  
13  
14  
15  
16  
17  
18  
19  
20  
21  
22  
23  
24  
25  
26  
27  
28  
29  
30  
31  
32  
33  
34  
35  
36  
37  
38  
39  
40  
41  
42  
43  
44  
45  
46  
47  
48  
49  
50  
51  
52  
53  
54  
55  
56  
57  
58  
59  
60
26. W. Y. L. Ko, H. G. Bagaria, S. Asokan, K. JiuHlina and M. S. Wong, CdSe tetrapod synthesis using cetyltrimethylammonium bromide and heat transfer fluids. *J. Mater. Chem.*, 2010, **20**, 2474–2478.
  27. W. W. Yu and X. Peng, Formation of high-quality CdS and other II-VI semiconductor nanocrystals in non coordinating solvents: tunable reactivity of monomers. *Angew. Chem, Int. Ed. Engl.* 2002, **41**, 2368–2371.
  28. T. Kippeny, L. A. Swafford and S. J. Rosenthal, Semiconductor nanocrystals: a powerful visual aid for introducing the particle in a box. *J. Chem. Educ.* 2002, **79**, 1094–1100.
  29. S. D. Bunge, K. M. Krueger, T. J. Boyle, M. A. Rodriguez, T. J. Headly and V. L. Colvin, Growth and morphology of cadmium chalcogenides: the synthesis of nanorods, tetrapods, and spheres from CdO and Cd(O<sub>2</sub>CCH<sub>3</sub>)<sub>2</sub>. *J. Materials Chem.* 2003, **13**, 1705–1709.
  30. S. F. Wuister, I. Swart, F. V. Driel, S. G. Hickeya and C. M. Donega, Highly Luminescent Water-soluble CdTe Quantum Dots. *NanoLett* 2003, **3(4)**, 503–507.
  31. S. F. Wuister and A. Meijerink, Synthesis and luminescence of (3-mercaptopropyl) trimethoxysilane capped CdS quantum dots *J. Lumin.* 2003, **102**,338–43.
  32. N. Joshi, K. Rawat, H. B. Bohidar, Coexistence of iso-nonergodic laponite gel and glass in 1-methyl-3-octylimidazolium chloride ionic liquid solutions. *J Phys. Chem. B.* 2014, **118(23)**, 6329-38.
  33. H. B. Bohidar (2002) In *Handbook of Polyelectrolytes*; H. S. Nalwa, S. Kumar, S. K. Tripathy, Eds.; American Scientific Publishers: C. A. Valencia Vol. II, 117144.
  34. K. Rawat, S. Agarwal, A. Tyagi, A. K. Verma, H. B. Bohidar . Aspect Ratio Dependent Cytotoxicity and Antimicrobial Properties of Nanoclay. *Applied Biochemistry and Biotechnology.* 2014; **174(3)**.
  35. A. Dey, A. Dasgupta, V. Kumar, A. Tyagi, A. K. Verma. Evaluation of the antibacterial efficacy of polyvinylpyrrolidone (PVP) and tri-sodium citrate (TSC) silver nanoparticles. *Int Nano Lett.* 2015. DOI 10.1007/s40089-015-0159-2
  36. T. Mosmann. Rapid colorimetric assay for cellular growth and survival: application to proliferation and cytotoxicity assays. *J Immunol Methods*, 1983, **65**, 55-63.

- 1  
2  
3  
4  
5  
6  
7  
8  
9  
10  
11  
12  
13  
14  
15  
16  
17  
18  
19  
20  
21  
22  
23  
24  
25  
26  
27  
28  
29  
30  
31  
32  
33  
34  
35  
36  
37  
38  
39  
40  
41  
42  
43  
44  
45  
46  
47  
48  
49  
50  
51  
52  
53  
54  
55  
56  
57  
58  
59  
60
37. H. Wang, H. Cheng, D. Wei, F. Wang. Comparison of methods for measuring viable *E. coli* cells during cultivation: great differences in the early and late exponential growth phases. *J Microbiol Methods.*, 2011, 84(1):140-3.
38. A. Kumar, A. K. Pandey, S. S. Singh, R. Shanker, A. Dhawan. Engineered ZnO and TiO<sub>2</sub> nanoparticles induce oxidative stress and DNA damage leading to reduced viability of *Escherichia coli*. *Free Radical Biology & Medicine*. 2011, 51, 1872–1881.
39. D. Y. Lyon; L. Brunet; G. W. Hinkal; M. R. Wiesner; P. J. J. Alvarez. Antibacterial activity of fullerene water suspensions (nC(60)) is not due to ROS-mediated damage. *Nano Lett.*(2008) 8:1539–1543.
40. M. D. Scott; S. R. Meshnick; J. W. Eaton. Superoxide dismutase-rich bacteria paradoxical increase in oxidant toxicity. *J. Biol. Chem.* 262:3640–3645; 1987.
41. C.E. Paradones, V.A. Illera, D. Peckham, L.L. Stunz and R.F. Ashman. Regulation of apoptosis *in vitro* in mature spleen T cell. *J. Immunol.* 1993, 151: 3521-3529.
42. S. S. Alam, N. S. Hassan and B. M. Raafat. Evaluation of Oxidatively Generated Damage to DNA and Proteins in Rat Liver Induced by Exposure to 99mTechnetium Radioisotope and Protective Role of *Angelica archangelica* and *Ginkgo biloba*. *World Applied Sciences Journal*. 2013, 24 (1): 07-17.
43. W. A. Kleinman, J. P. Ritchie. Status of glutathione and other thiols and disulfides in human plasma. *Biochem Pharmacol.* 2000; 60:19-29.
44. O. H. Prasad, A. Navya, D. Vasu, T. Chiranjeevi, M. Bhaskar, K.V. Sreedhar Babu P.V.G.K. Sarma. Protective effects of *Prosopis juliflora* against *Staphylococcus aureus* induced hepatotoxicity in rats. *Int J Pharm Biomed Res.* 2011, 2 (3): 172-178.
45. J. Lovrić, H. S. Bazzi, Y. Cuie, G. R. Fortin, F. M. Winnik, D. Maysinger. Differences in subcellular distribution and toxicity of green and red emitting CdTe quantum dots. *J Mol Med.* 2005, 83:377–385
46. Lars-Oliver Klotz Klaus-Dietrich Kröncke and Helmut Sies. Singlet oxygen-induced signaling effects in mammalian cells. *Photochem. Photobiol. Sci.*, 2003,2, 88-94
47. E. Cabiscol, J. Tamarit, J. Ros. Oxidative stress in bacteria and protein damage by reactive oxygen species. *Internatl microbiol*, 2000, 3:3–8.

1  
2  
3 48. A. Tyagi, S. Agarwal, A. Leekha and A. K. Verma. Effect of Mass and Aspect  
4 Heterogeneity of Chitosan Nanoparticles on Bactericidal Activity. *International Journal*  
5 *of Advanced Research*. 2014, 2, 8: 357-367.  
6  
7  
8  
9  
10  
11  
12  
13  
14  
15  
16  
17  
18  
19  
20  
21  
22  
23  
24  
25  
26  
27  
28  
29  
30  
31  
32  
33  
34  
35  
36  
37  
38  
39  
40  
41  
42  
43  
44  
45  
46  
47  
48  
49  
50  
51  
52  
53  
54  
55  
56  
57  
58  
59  
60